DESIGNANDDEVELOPMENTOF AT89C2051 BASED ACOUSTICS TOMOGRAPHY SYSTEM

A Thesis submitted in partial fulfillment of the Requirement for the award of degree of

Master of Engineering

in

Electronic Instrumentation and Control

Submitted by

Hitesh Nagpal

Regd. No 801251008

Under the Guidance of:

Dr T.K. Saxena

Chief Scientist and Head

Vibration, Ultrasonic and Acoustic Standards and Instrumentation Cell
CSIR-National Physical Laboratory
Dr. K. S. Krishnan Road New Delhi

Dr. Ravinder Agarwal

Professor

Department of Electrical& Instrumentation Engineering
Thapar University, Patiala
Punjab

Department of Electrical and Instrumentation Engineering

Thapar University

(Established under the section 3 of UGC act, 1956)

Patiala, 147004, Punjab, India

July 2014

DECLARATION

I hereby certify that the work which is being presented in this Dissertation entitled, **"DESIGN AND DEVELOPMENT OF AT89C2051 BASED ACOUSTICS TOMOGRAHY MODEL"** in partial fulfillment of the requirements for the award of degree of masters of engineering in Electrical & Instrumentation Engineering Department, Thapar university, Patiala, is an authentic record of my own work carried out under the supervision of**Dr T.K. Saxena**, Chief Scientist National Physical Laboratory, New Delhi and **Dr. RavinderAgarwal**, Professor, HOD of Electrical and Instrumentation Engineering Department, Thapar University, Patiala, Punjab.

Date: 17/07/14

Hitesh Nagpal

Hitesh Nagpal
Roll No 801251008

I certify the above statement made by the candidate is correct and true to best of my knowledge and belief.

Date:

T.K. Saxena

Dr. T.K. Saxena
Chief Scientist and Head
Vibration, Ultrasonic and Acoustic
Standard and Electronics and
Instrumentation Cell
CSIR-National Physical Laboratory
Dr. K. S. Krishnan Road
New Delhi- 110 012

Dr. RavinderAgarwal
Professor H.O.D
Department of Electrical &
Instrumentation Engineering
ThaparUniversity, Patiala
Punjab.

Countersigned By

Dr. RavinderAgarwal
Head of Department
Department of Electrical &
Instrumentation Engineering
Thapar University, Patiala
Punjab.

Dr. S.K. Mohapatra
Dean of Academic Affairs
Thapar University
Patiala
Punjab.

सी. एस. आई. आर. - राष्ट्रीय भौतिक प्रयोगशाला
CSIR - NATIONAL PHYSICAL LABORATORY
(Council of Scientific & Industrial Research)
(वैज्ञानिक तथा औद्योगिक अनुसंधान परिषद्)
डा० के. एस. कृष्णन् मार्ग, नई दिल्ली-110012
Dr. K.S. Krishnan Marg, New Delhi-110012

Ref: NPL/TKS/HN/TRAIN/01/2014 **Dated:** July 14, 2014

CERTIFICATE

This is to certify that *Mr. Hitesh Nagpal S/o Mr. Rakesh Nagpal* student of M.E. (Instrumentation and Control) Fourth semester, Roll No 801251008, Thapar University, Patiala, Punjab, has successfully completed his six months training from January 01, 2014 to July 14, 2014 under my supervision. Title of his project was *"Design and Development of 89C51 based Acoustic Tomography"*.

During his project work Mr. Hitesh has taken keen interest in learning every aspect of 89C51 microcontroller, 8051 assembly language, designing and fabrication of the circuit related to his project, Visual BASIC 5.0 language and EIDORS (Matlab).

I wish him all the success in life.

T.K. Saxena

(Dr. T.K. Saxena)
Chief Scientist and Head
Acoustic, Ultrasonic & Vibration Standards
and Electronics & Instrumentation Cell

Fax / फैक्स : 91-11-45609310
Director Office : 45609201 / 45609301
COA's Office : 45609203
COS&P's Office : 45608367
SPO's Office : 45609326

ई-मेल : root@nplindia.org
E-mail : root@nplindia.org
वेबसाईट/Website : www.nplindia.org

Acknowledgement

With deep sense of gratitude I express my sincere thanks to **Dr. Prakash Gopalan,** Director of Thapar University, Patiala. To my esteemed and worthy supervisors, **Dr. Ravinder Agarwal** Head of Department of electrical & Instrumentation Engineering, **Dr T.K. Saxena**, Chief Scientist and Head Vibration, Ultrasonic and Acoustic Standard and Electronics and Instrumentation Cell, NPL New Delhi for their valuable guidance in carrying out this work under their effective supervision, encouragement, enlightenment and cooperation. Their feedback and editorial comments were also invaluable for writing of this thesis.

I express my sincere thanks to Prof. R.C. Budhani, Director NPL for providing me the opportunity to work at the NPL. I would also like to thanks Dr. Rajeev Chopra, Head HRD, NPL and Mr.Dharamvir, HRD NPL for their support and guidance.

I am also thankful to Mr. Naveen Garg, Ms. Priyanka Jain and Ms. Poonam Sethi Bist for their full co-operation and timely help.

A special thank is to my beloved family, to my father, my mother, my brother and sister for their unlimited love and support.

Finally, I would dedicate this work to my grandfather, the most solicitous person to my M.E Dissertation. Because of him, I did not give up even in the hardest time.

Place: Thapar University, Patiala Hitesh Nagpal

801251008

ABSTRACT

Acoustics Tomography is an imaging technique that deals with transmission, reception, control, production and effects of sound. It can be used in Medical, Geophysical and Industrial fields for imaging the internal parts of human body, looking beneath the earth and process control respectively. Propose topic of dissertation is the design of a laboratory driven automotive hardware structure for data analysis of sound power level of a sound source, using reverberation and anechoic test rooms with specified acoustical characteristics and make software to represent the distribution pattern with different sound power levels at different frequencies.

In this dissertation work Acoustics Tomography model is designed and developed around microcontroller 89cLP2051 and Op-Amp OP07 and software part were developed with VB.10 and EIDORS Tool-kit for MATLAB R2012a.The system was tested and results were obtained in two sound testing chambers i.e. Reverberation and Anechoic chambers in National Physical Lab. , New Delhi. The obtained results are when compared with the data obtained by conventional method using microphone, proposed system model was found as an effective way to validate these sound chambers. Thus the system model can be used as a prototype in the laboratory for the evaluation of Acoustics Tomography technique.

TABLE OF CONTENT

Declaration ii

Acknowledgement iii

Abstract v

1: **CHAPTER ONE** 1-5

Acoustic Tomography: An Introduction 1
1.1Introduction to Acoustic Tomography 1

2 **CHAPTER TWO** 6-5

Literature Review 6
2.1 Introduction 6

2.2 History of A.T 8

2.3 Image Reconstruction Method 11

2.3.1 Solving the inverse problem 11

2.3.2 Ray tomography 12

2.3.3 Waveform tomography 14

2.3.4 Diffraction Tomography 15

3 **CHAPTER THREE** 16-24

Image Reconstruction Software 16
3.1 Introduction 19

3.2 Software Architecture 19

3.2.1 Object Structure 19

3.2.2 Forward Model 19

3.2.3 Data 22

3.2.4 Image 23

3.2.5 Reconstruction 23

3.3 EIT Processing 24

4 **CHAPTER FOUR** **25-30**

Hardware Description 4.1 25
Model Components 25

4.1.1 Loudspeaker 25

4.1.2 OP-07(Operational Amplifier) 26

4.1.3 Microcontroller AT89c2051 26

4.1.4MAX 232 27

4.1.5 IC 74HC244 (Tri-state Octal Buffer/ line Driver) 28

4.1.6 IC SN7407 (HEX BUFFERS/ DRIVERS) 29

4.2Tomography controller 29

5 **CHAPTER FIVE** **31-36**

Result and Discussion 31
5.1 Results 31

5.2 Conclusion 35

6 **CHAPTER SIX** **37**

Future Work 37

6.1 Variable Height 37

6.2 Increasing Sensor Numbers 37

6.3 Clinical Experiment 37

7 CHAPTER SEVEN **38-42**

References 42

LIST OF FIGURES

Sr. No Page No.

1. Figure 2.1: Generalized AT System. 7

2. Figure 3.1: The Structure of the EIDORS Forward Model Object **3.** 20

Figure 3.2: The structure of the EIDORS Data Object. 22

4. Figure 3.3: The structure of the EIDORS Image Object. 23

5. Figure 3.4: Finite Element Mesh and Electrodes used to Solve Forward Problem. 24

6. Figure 4.1 Block diagram representation of the system model 25

7. Figure 4.2 OP07 pin description 26

8. Figure 4.3 pin description of MAX 232 **9.** 27

Figure 4.4 Pin description of 74HC244 28

10. Figure 4.5 pin description of 7407 29

11. Figure 4.6 Block diagram of power supply **12.** 30

Figure 4.7 Block diagram of system model 30

13. Figure 5.1 Image of developed system 31

14. Figure 5.2 Speaker as a sensor 31

LIST OF TABLES

Sr. No Page No.

1. Table 1.1 Different applications of Acoustics Tomography 3-4

2. Table 4.1: Function of each driver of MAX232 27

3. Table4. 2: Function of each receiver of MAX 232 **4.** 27

Table 4.3 TRUTH TABLE for 74HC244. 28

5. Table 5.1 Results obtained of standard deviation at Variable frequencies 32

6. Table 5.2 Results obtained by conventional method using microphone. 33

7. Table 5.3 Comparison graph of conventional system and proposed automatic model 34-35

CHAPTER ONE

ACOUSTICS TOMOGRAPHY: AN INTRODUCTION

Acoustics is defined as the study of science that deals with the transmission, reception, production, control and effects of sound (as defined by Merriam-Webster)[1] and Tomography refers to imaging by sections or sectioning, through the use of any kind of penetrating wave [2].The device used in tomography is called as Tomograph and the image produced is called as tomogram**.**

Acoustics Tomography (AT) belongs to a family of computerized tomography imaging technique such as ultrasound tomography [3] and electromagnetic tomography (EMT)[4]. This technique can be used to explore the distribution pattern of sound waves, by measuring its boundaries. Usually a set of sound pressure level (SPL) is acquired from the subjected frequency pattern. In principle, measuring SPL at different frequencies results in image formation of pattern distribution along the region. The frequency distribution lies in the range of 50 Hz to 10000 Hz. A typical AT system is a compact set of unit mainly consists of a set of hardware structure, with data acquisition unit, sound source and a PC with software codes.

Soft-Field modalities such as AT when compared to Hard-Field tomography method like X-rays computer tomography (CT) are found to be much more difficult and complex in terms of widely established high resolution imaging [5]. An x-ray CT scanner works when series of parallel beam of x-rays are projected over the body under observation from certain source and detector placed on the other side of test body. Detector receives the rays and forms an image corresponds to the test body. The process can be repeated by repeating the procedure, by varying the position of source and detectors. By the sequence of images thus formed can be reconstructed as a final image using suitable algebraic or analytic algorithms. Also these techniques are proved to be very efficient for reconstruction of images and in terms of calculations and computations of data obtained. Another reason for this methods affectivity is the property of x-rays that they propagates in straight line only, thus the absorption of rays at any point is purely independent of surrounding areas. On the other hand, AT uses such a technique that also works in accordance with CT method for solving

inverse problems, involving sound signals. It can be concluded that AT explores the volume of material under observation when placed along the surface. But Unlike the X-rays CT phenomenon, sound behaves purely like waves with such long wavelength and can work with very low frequencies and thus describes the boundaries appropriately using laplacian equations.

The boundary values are sometimes not easy to be determined as the distribution pattern parameters are not always uniform. And thus this makes the reconstruction problem uneasy sometimes. But mostly the localization algorithm in AT uses homogenous background. However the structure under investigation may be inhomogeneous, i.e. the structure may contains heterogeneities and thus limiting the accuracy of source localization algorithm.

In order to overcome the drawbacks of source localization algorithm in AT, travel time of wave can be combined with AT by combining the emission sources as acoustic points. In this process an update of emission point is required after each tomographic inversion, thus results in iterations with source localization and tomography. This process works in accordance with the principle of geo-physics, to determine the source of earthquakes and also used for tomographic imaging of earth's interior [6]. Another drawback of AT technique is its poor resolution of reconstructed image, as compared to well established scanner with good resolution it provides a reliable, portable, real-time and cost effective imaging tool. The weak spatial resolution is due to ill-posedness in image reconstruction, as large measurement declines in quality of image.

Thus in an abstract way; obtained images can be considered as a source of information, explaining interior properties of some particular subject. Depending upon the area of application and obtained specifications. AT can sometimes be proved as an optimum cost effective imaging tool. At present there are numbers of AT systems performing imaging in a variety of applications.

Few examples of approaches using AT are shown:

1. Seismic imaging: Using acoustic signals for lithosphere simulation results much finer details over the conventional methods of developing numerical model and ray based reconstruction method [7, 8].

2. Forestry: AT is increasing its demand to measure the properties of trees by applying cross-sectional sound and by then making its reconstruction image. It's basically used to determine health of a tree. Experiment was carried by a string of sensors tied around a tree and transmission tomography results in imaging of tree trunk. This is an effective way to differentiate between a healthy and a decaying tree [9].

3. Atmospheric imaging: Low frequency acoustic source arrays are applied to get image of wind direction and temperature distribution in atmosphere. The setup includes a string of sensors around the heat source [10].

4. Medical imaging: A very safe, simple and low cost system can be designed using AT to get human abdominal cross sectional sound speed image for the diagnosis of metabolic syndrome [11]. Another application in medical field is the detection of breast cancer by developing a clinical prototype. Sound speed images results from arrival acoustic signal. Studies have showed that tumor have enhanced sound speed than normal tissues [12, 13].

The AT systems shown in the above areas have made contribution in preparing real-world laboratory data and are also commercialized in some areas also. Examples of real-world systems are be listed in a TABLE-I.

Table 1.1 Different applications of Acoustics Tomography

Area of application	**Imaging Targets**	**Transducer Frequency**
Geophysical	Oil /ore deposits	1 Hz – 2 KHz
Medical	Tissues /lesions	1 – 5 MHz
Industrial	NDT Flaws	0.5 – 150 MHz
Forestry	Tree decay	10-100 KHz
Agriculture	Spoilage / insects	0.5 - 3 KHz

Meteorology	Temperature and wind velocity	40 KHz
Process	Air/liquid flows	1-3 MHz
Oceanography	Ocean monitoring	100 – 200 KHz
Civil	Infrastructure Flaws	1 – 500 KHz

In many practical applications of AT, objects can be confined in either 2-D plane or 3-D volume and the taken measurement are generally made in 1-D or 2-D space respectively. The setup for AT typically involves an array of transducers or in some cases rotating a transducer around the object. Acoustic waves are made to fall on an object by a probe and are collected at the other end through a receiver, the interaction of sound waves and object is our aim of measuring.

The measurements are then recorded and then reconstruction of image tomography is done using some set of mathematical tools. Ordinarily QT sensors are employed in experiments consisting of sound or ultrasound transducers. These are highly efficient transducers, converting electrical energy into mechanical energy and vice-versa. Generally a single transducer is used as both transmitter and receiver i.e. same transducer can be used in switching between two models. For a high depth of ray coverage, number of transducer are distributed along the space and the travel time between each source and receiver is measured. The resulting tomographic image illustrates the locally varying wave speed diffusion inside the specimen. On second thought, the amplitudes of transmitted time variant signal at the receiver end can be measured and the deflections in the attenuation can be reconstructed. However, the later method demands large number of transducers coupling conditions.

With the basic principle explained in above sections, it is now easy to unfold the concept of AT transmission inside the specimen as acoustic point sources. When the numbers of point sources are large, the depth of coverage of rays is high. So the number of available rays paths and the depth coverage id dependent on the number of transducers. E.g. for some small array of sensors (n=8), the location of point sources are managed such that to achieve the highest uniformity, when working in homogenous conditions.

Another important advantage of AT is in an aircraft, usually the majority of AT events is produced by sources of interventions like joints and a great effort is required to divide these unwanted signals from wanted signals generated by other defects or cracks. In AT, these unwanted sources can also be used for tomographic imaging provided that they can also be treated as transient point sources and provides information about the location of active regions, AE tomography visualizes both, active and non-active regions of the specimen. Therefore, acoustically “passive” defects in the structure can also be identified in principle.

Here, towards the accomplishment of AT’s introduction, it is important to mention that this system represents a purely algorithmic tool for image reconstruction using raw data only i.e. no supplementary expenses regarding data acquisition are necessary.

CHAPTER TWO

LITERATURE REVIEW

2.1 Introduction

Acoustics Tomography (AT) is a technique for mapping the distribution of acoustic sources within some medium. The sound transmission information is obtained from measurement of Sound pressure level (SPL) and/or frequency on the periphery of the region as a result of externally applied sound. Images can be obtained from the peripheral data with the use of an algorithm**.** In the opposing limits of wavelength, acoustics have played a major role in geophysical applications on the one hand and in medical ultrasound imaging on the other. In contrast to X-rays, acoustic waves interact strongly with materials through which they propagate, through processes such as refraction, reflection and diffraction. The interactions can be very strong in heterogeneous media such as human tissue. Tomographic reconstructions of acoustic data therefore require much more sophisticated modeling of acoustic wave propagation often involving highly non-linear inversions. One of the research subject is acoustic computerized tomography is in the field of healthcare and daily life environment. This technique can provide the human abdominal cross sectional sound speed image for use in the metabolic syndrome diagnosis. The diagnosis of metabolic syndrome has now come up as a serious warning signal of three major lifestyle related diseases i.e. diabetes, brain infarction, and cardiac infarction; for this reason an abdominal examination by an X-ray CAT scan is now one of the regular health check-up test. However, an X-ray CAT scan includes the risk of radiation exposure, and is not recommended for frequently-conducted examinations. Furthermore, because of the expensive equipment, these systems are only installed in large hospitals. As an outline to tackle these problems, AT has proved to be a small-sized, safe and inexpensive method for abdominal examination based on ultrasound tomography, which can be done in the home or at a clinic level. This technique proves helpful in reconstruction of an image of the sound speed distribution in the abdominal cross section and this method is applied to the acoustic wave travel time for data transmitted and received at the different locations on the abdominal body surface. This technique use the properties of slow sound speed in fat regions whereas fast sound speed in

muscles and other regions; the basic principle is to estimate and measure the visceral fat area from the reconstructed sound speed image.

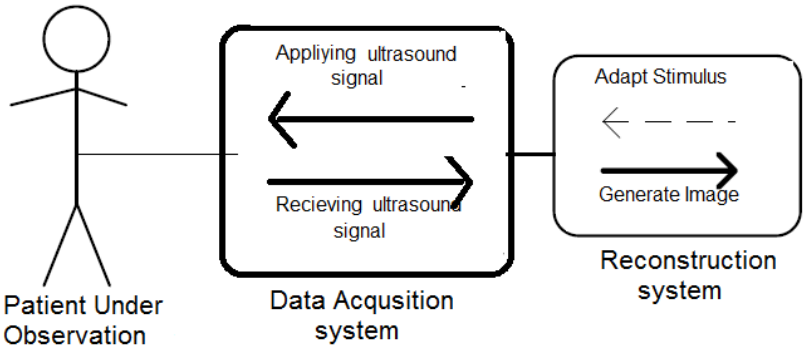

Figure 2.1: Generalized AT System.

A generalized AT system can be shown in the form of block diagram as above in Figure 2.1. In the above figure, an array of transducer is placed around the particular body part of patient under observation. When the signal of sound waves is made to fall on the patient from the transmitter end, and some signal is received at the other end by the receiver, this transmission/reception forms the data acquisition block; because the data is obtained in this block. Next and the last block is reconstruction block, here suitable algorithm used to form the image of the subject under observation. The main difference from Other Methods is, Ultrasound tomography conducts reconstructive calculations to make a sound speed physical parameter image of an object as a solution for a physical equation. The data is obtained from multidirectional and multipath observations, and the medium parameters. Formerly, it has been difficult to measure the living tissue using sound speed in human body by non-invasive technique. The ultrasound tomography method is an effective measure to hold this purpose. As a result, for body sites with no obstacles (e.g. lungs or the bones) to sound waves, clinical equipment has been developed to diagnose such diseases as breast cancer. But, in the case of a cross sectional imaging for the human abdomen, the spinal cord presents an inverse problem as unfavorable condition. The path rays passing through the spinal cord dose not makes the proper imaging, acting as an obstacle, so it became difficult to use this method. So to deal with this issue, low-frequency ultrasound waves with several hundred kHz bands were used. Supplementary, a smoothed path Algebraic Reconstruction Technique (ART) was proposed, capable as a corrective measure in such unfavorable conditions.

By this means, it became possible to reconstruct the abdominal cross sectional image, by the use of small amount of transmission/reception path data, which restricts path rays passing through the spinal cord between the abdominal cross section [14, 15, 16]. The speed of image reconstruction is limited by the speed of the data acquisition system algorithm. Data acquisition and image reconstruction has to be fast enough to allow quick real-time view, and this can be achieved using source localization method. This method have recently become fast enough to retrieve data and reconstruct at near video rates. AT also provides the potential to meet the requirements for a low-cost, safe and real-time imaging system which also provides good contrast between tissues and causes no harms to the tissue cells.

2.2 History of AT

Imaging with acoustic waves has made great advances in recent decades. Acoustics Tomography have played a major role in geophysical applications on the one hand and in medical ultrasound imaging on the other. The basic idea of applying this method in medical treatment was proposed in the early 1980s, and since then, researchers have invented many different techniques. As discussed in pervious chapter that unless X-rays used in conventional CT, sound is purely wavelike tomographic technique that process only sound related data. In an inhomogeneous medium, ultrasound pulses do not travel in straight lines, and thus complicates the tomographic calculations and placing extra burden on the computational requirements. The requirement for a high level of computing power and associated data processing tools has been a major historical factor in limiting the development of AT compared to CT and other tomographic methods. However, in recent years, because of increasing processing speed of both computers and electronics, the scenario has changed dramatically, thanks to the exponential increase of computing power which has largely followed Moore's Law. Over the past 30 to 40 years, computing power has increased by a factor of 10 million and at the same time, the processing power of electronic devices has also increased about 10 million fold leading to massive parallelization of data acquisition and the ability to process large amounts of data. These two parallel trends have enabled the development of tomographic systems containing large numbers of transducers (sensors). In the area of medical imaging, for example, large transducer arrays are bringing about the

realization of ultrasound tomography (UST) systems that are gaining clinical applications.

Source Localization

In many cases, AE localization is done under the assumption of a homogeneous background medium and thus, $c_i = c$ = constant for all rays sensors. Let us presume we have i = 1,…, N sensors and the P-wave arrival times of a single AT event have been determined by using an expropriate algorithm. In a first approximation the arrival time at sensor i is given by:

$$t_i^A = \frac{\left|\underline{r}_i^S - \underline{r}\right|}{c_i} + t = \frac{\sqrt{\left(x_i^S - x\right)^2 + \left(y_i^S - y\right)^2 + \left(z_i^S - z\right)^2}}{c_i} + t \tag{2.1}$$

where $\underline{r}_i^S = (x_i^S, y_i^S, z_i^S)$ is the known position of sensor i and $\underline{r} = (x, y, z)$ is the unknown location of the AE event to be determined by the localization algorithm; t represents the source time of the AT event and is usually measured relative to a prompt level.

Eq. (2.1) is based on a simple straight ray model for the source-sensor travel path. In this context c_i is the mean effectual wave speed along ray i . On the other hand, in a inhomogeneous medium the effectual wave speed can be different from one ray to another, i.e. $c_i \neq c_j$ for $i \neq j$, in general.

In Eq. (2.1) we have four unknown elements, i.e. the three source coordinates x, y, z and the source time t. So, at least four different sensor arrival times and thus four equations are needed to solve the basal system. Since Eq. (2.1) is a nonlinear system of equations, a closed precise solution is not available in general and thus, it has to be solved by an iterative method.

For that reason we begin with some initial values x_0, y_0, z_0, t_0 and assume that the effectual wave speeds c_i are all known. Again by using the same straight ray model as described above it is now easy to calculate the theoretical arrival times using Eq. (2.1) In general, these calculated theoretical times will be different from the measured arrival times t_i^A From the differences $\Delta t_i^A = T_i^A - t_{i,0}^A$, the correction values for the

next iteration Δx, Δy, Δz, Δt can be obtained. Since the measured arrival times can be written as a function of x, y , z, and t.

$$T_{i\,A} = f_i\,(x, y, z, t) = t^A_{i,0} + \Delta t_{iA} = t^A_{i,0} + \frac{\partial fi}{\partial x}\,\Delta x + \frac{\partial fi}{\partial y}\Delta y + \frac{\partial fi}{\partial z}\,\Delta z + \frac{\partial fi}{\partial t}\Delta t \tag{2.2}$$

The arrival time difference Δt_i^A is expressed as total differential of f_i. In matrix form we have

$$\begin{pmatrix} \Delta t_1^A \\ . \\ . \\ . \\ \Delta t_N^A \end{pmatrix} = \begin{pmatrix} \frac{\partial f_1}{\partial x} & \frac{\partial f_1}{\partial y} & \frac{\partial f_1}{\partial z} & \frac{\partial f_1}{\partial t} \\ . & . & . & . \\ . & . & . & . \\ . & . & . & . \\ \frac{\partial f_N}{\partial x} & \frac{\partial f_N}{\partial y} & \frac{\partial f_N}{\partial z} & \frac{\partial f_N}{\partial t} \end{pmatrix} \cdot \begin{pmatrix} \Delta x \\ \Delta y \\ \Delta z \\ \Delta t \end{pmatrix} \tag{2.3}$$

or in short, $\underline{\Delta t^A} = F \cdot \underline{\Delta s}$ (2.4)

where $\underline{\Delta t}^A$ and F are known while $\underline{\Delta s}$ is unknown. If the number of sensors is N = 4, the solution of Eq. (4) is well-defined, as:

$$\Delta s = F^{-1} \cdot \Delta t^A \tag{2.5}$$

If N > 4, the problem is over-determined. In this case a least-square approximation with regard to arrival time differences is given by the normal equation:

$$\Delta s = (F^T \cdot F) \cdot F^T \cdot \Delta t^A \tag{2.6}$$

Using the results from Eq. (2.6) , the upgrade of source coordinates and source time from iteration 0 to iteration 1, or more general from iteration k to k+1 can now be demonstrated as:

$$X^{(k+1)} = x(k) + R\Delta x$$
$$y^{(k+1)} = y(k) + R\Delta Y$$
$$z^{(k+1)} = z(k) + R_Z\,\Delta z$$
$$t^{(k+1)} = t\,(k) + R_t\,\Delta t$$

where the R_j's with $0 \le R_j \le 1$ and j = x, y, z, t are relaxation parameters. In order to ensure convergence of the iterative method, values of R ≈ 0.1 are commonly used.

2.3 Image Reconstruction Methods

In an inverse problem one wishes to find *p* such that,

$$d = G(p) \tag{2.7}$$

where G is an operator explaining the relationship between the data d and the model parameters *p*, and is a depiction of the physical system. The operator *G* is called as the forward operator. Many a time, in practical applications the object can be restricted either to a 2-D plane or a 3-D volume while the measurements are made in 1-D or 2-D space respectively. The measurements are then recorded and used to construct an image tomographically. An array of transducers is generally more exorbitant to build and field but it offers the possibility of either electronic multiplexing or a parallelized system that provides data channels for many or all elements, thereby greatly speeding up the data acquisition process. There is therefore a trade-off between the cost and speed correlated with any AT implementation.

2.3.1 Solving the inverse problem

Obtained by the AT system and by the sophistication of the reconstruction algorithm. The latter is defined by how well the physics of the sound propagation are modeled. Generally, the simpler the wave-based suppositions the faster an algorithm can run but the lower the quality of the final image. Therefore, a trade-off exists between reconstruction speeds and image quality. This trade-off can be understood by discussing the wave propagation theory and its computational executions as summarized below. Sound propagates according to the acoustic wave equation as:

$$\nabla^2 p - \frac{1}{c^2}\frac{\partial^2 p}{\partial t^2} \tag{2.8}$$

where ∇^2 is the Laplace operator, p is the acoustic pressure (the local deviation from the ambient pressure), and where c is the speed of sound. The latter can also be defined as:

$$c^2 = \frac{k}{\rho}$$

where ρ is the material density and K is the compressibility constant. The solution for a spherical wave in a homogenous medium is stated as:

$$p(r , k) = \frac{Ae^{\pm ikr}}{r} \tag{2.10}$$

Where k is the wave number and A is the amplitude of the wave which falls off with radial distance travelled r. It is evident that the propagation of the acoustic wave is sensitive to the material properties of density and stiffness. Therefore, for a variegated medium, the solution is much more composite and requires algorithmic computations. Moreover, both transverse and longitudinal waves are supported in any real system. However, most AT implementations depend on measurements of the longitudinal wave since it propagates much more speedily and decays relatively slowly. The longitudinal waves can also undertake mode conversions creating surface waves, such as those cited to as the "whispering gallery". A full solution to the wave equation is therefore computationally intimidating given the complexity of the physics being described. Most reconstruction methods therefore make simplifying assumption to make the problem manageable.

2.3.2 Ray tomography

For finite bandwidth sound waves used in acoustic imaging, energy travels from transmitter to receiver along a hollow banana shaped volume which can be represented as a “Banana– Donut” .The center width of the “Banana - Donut” for dominant the frequency is the width of the first Fresnel zone, $\sqrt{\lambda L}$, where λ is the wavelength and L is the distance between transmitter and receiver. In ray theory, this volume is slumped into an infinitesimal line (ray path) by assuming the infinite frequency approximation, similar to what is assumed for geometrical optics. The straight ray estimation is similar to the presupposition made for CT reconstructions which assume X-rays travel in straight lines. Thus, every transmitter is connected to every receiver by a straight line. The spatial resolution of the reconstructed images is poor because the straight ray estimation does not take into account the refraction of the waves as they pass through an inhomogeneous medium. This blurring can be decreased by taking refraction into account when reconstructing the images by allowing for rays to distort as they propagate from transmitter to receiver. [17, 18, 19, 20]

Bent ray tomography relies on the knowledge that refraction is governed by changes in sound speed. The initial model of sound speed can be homogeneous or heterogeneous. The model is used to bend the rays as they propagate from one pixel to the next. The detected ray path and predicted arrival times are used to generate the next sound speed model which allows for more accurate bending. The process is repeated until convergence is achieved. The net effect of bending the rays is to compensate for the refractive effects and thereby reduce artifacts and improve the spatial resolution [21]-[24].

Ray-based Transmission algorithms

A typical transmission algorithm has 3 components:

Data processing. Before performing ray-based sound speed tomography on the acquired acoustic data, the time-of-flight (TOF) for each received waveform needs to be picked. In other words, the onset time of the signal arriving at receiver needs to be determined. The picked TOFs are used to reconstruct sound speed images. To determine the TOF for each waveform, either manual picking or some forms of automatic picking can be exploited. Automatic pickers are required when large volumes of data are collected, as in medical imaging. Before performing ray-based attenuation tomography on the acquired data, the attenuation data for each received waveform needs to be calculated. Various authors present different ways to determine attenuation data from the received waveforms [25, 26, 27].

Forward model. In straight ray tomography, the propagation paths of sound waves are assumed to be straight lines. In bent ray tomography, 2-D wave propagation is governed by the *eikonal equation*. The eikonal equation can be obtained from the wave equation in the limit of infinite frequency. To solve the inverse problem, a regular rectangular grid model is created on the image plane, whose boundaries enclose the acquisition geometry. The Eikonal equation is solved to obtain a travel-time map for each source (transmitter) position which is later used to calculate travel-time gradients for ray tracing. A ray is back-propagated from receiver to transmitter based on either a straight ray path (straight ray tomography) or a travel-time gradient method (bent ray tomography) . The traced ray paths serve as a sensitivity matrix in the inverse process [28].

Inversion. This is a linear problem for straight ray tomography since the matrix is fixed through the whole inverse process. The problem becomes nonlinear when we take the ray bending into consideration, in which case the matrix depends on the current sound-speed model. For bent ray tomography, ray paths are copied on the updated sound speed model after each iteration.

The iteration continues until the solution converges. A simple stopping criterion is that the cost function for the current iteration is not significantly improved from the previous iteration [29, 30].

2.3.3 Waveform tomography

With ever-increasing computational power the ability to solve the wave equation is being realized. Solutions are now possible, for both sound speed and attenuation [34]. The advantage of this approach in light of the computational burden is that it allows for diffraction as well as a better correction for refractive effects. Furthermore, by utilizing all of the recorded wave information (as opposed to the arrival time of the signal) the method has the potential to increase image contrast while suppressing artifacts. The limiting resolution of $\Lambda/2$ is up to an order of magnitude better than ray tomography [35]. We can observe that the quality of the reconstruction is significantly enhanced compared to ray-based reconstructions. In particular, the heterogeneities in the image are well resolved and have sharp boundaries. Waveform tomography reconstruction methods have been formulated in the time domain and in the frequency domain. The latter usually allows for a simpler formulation of the problem since convolution and differential operators are mapped to multiplications. The reconstruction process is similar to ray tomography. We start from an initial model of the unknown parameters (sound speed, attenuation) and solve a forward problem. The solution of this forward problem is a set of simulated waveforms recorded at the transducer locations. The residual between the recorded waveforms and the measured ones is then used to update iteratively the unknown parameters until convergence. Forward modelling is usually achieved by means of finite difference or finite element methods. These methods must be accurate enough to avoid numerical dispersion and to properly account for the boundaries of the simulation area (e.g., absorbing boundary conditions) [36]. For a given accuracy, the size of the model typically scales linearly with the frequency of the probing pulse. Complexity can be lowered using

approximations. It can also be addressed by means of efficient parallel implementations [37]. However, this issue remains a challenging one, especially in medical imaging applications where reconstruction time must be kept at a minimum to keep a high patient throughput. Convergence to the correct cycle of the waveform requires an accurate initial model, especially at high frequencies. One approach is to start from an initial model obtained using ray tomography, and to sequentially drive the iterative algorithm using waveform components from low to high frequencies.

2.3.4 Diffraction Tomography

As noted above, waveform tomography is computationally intensive while ray tomography is fast but provides inferior spatial resolution. Investigators have sought simplified forms of the wave equation to reduce the computational burden while avoiding the ray approximation. The most common simplifying assumptions are known as first Born approximation and first Rytov approximation [31]-[33].

First Born approximation: In this approach, the wave equation is simplified by assuming that scattering is weak and there is no multiple scattering as the wave propagates from the transmitter to the receiver. The first Born approximation assumes the heterogeneity in the propagating medium perturbs the total wave field. It consists of taking the incident wave field in place of the total wave field as the driving wave field at each scatterer. This approximation is accurate enough if the scattered wavefield is small, compared to the incident wave field. It breaks down if the scattered wave field becomes large relative to the reference wave field. Consequently, this method achieves high resolution but fails to properly reconstruct images with more than a few percent contrast differences. In most clinical applications, it is tantamount to assuming that the object being imaged can be inhomogeneous but with very small contrast variations.

First Rytov approximation: The first Rytov approximation starts by assuming the heterogeneity in the medium perturbs the phase of the scattered wavefield. This approximation is valid under a less restrictive set of conditions than the first Born approximation .The validity of first Rytov approximation is governed by the change in scattered phase over one wavelength not the total phase. In other words, first Rytov approximation is valid when the phase change over a single wavelength is small (a few percent). Unfortunately, most applications violate this assumption.

CHAPTER THREE

IMAGE RECONSTRUCTION SOFTWARE

3.1 Introduction

EIDORS (Electrical Impedance and Diffuse Optical tomography Reconstruction Software) is a software suite for image reconstruction in electrical impedance tomography (EIT) and diffuse optical tomography (DOT). But it can also be used in Acoustics tomography (AT) reconstruction. It is basically a modifiable software for image reconstruction of electrical or diffuse optical data. Such software also facilitates research and development in other fields by providing a reference implementation according to which new developments can be made, and provides functioning software base from which new ideas may be built and tested in other fields. By providing source code also facilitates close examination of algorithms and their implementation in many researches. The original EIDORS (version 1) software [38] is based on software from the dissertation of Vaukhonen [39]. It works in accordance with MATLAB package for two-dimensional mesh generation, solving of the forward problem and reconstruction and display of the images. In order to solve 3D reconstruction models, a new project, EIDORS3D (version 2), was build based on the software developed for the dissertation of Polydorides [40]. EIDORS software packages have ability to solve basic and complex numerical and algorithmic foundations, but shared very little software code.

A simplex based finite element representation is used in modelling any medium under investigation, and images were reconstructed using regularized inverse techniques. Since the publication of EIDORS3D, several patterns of use have been noted. To best understand the software, download the software, run the provided demonstration examples, and make modifications according to the requirement in the demonstration examples and the software internals to meet their needs. Because of the insufficiency of a modular software structure of EIDORS3D, changes tended to be made into the code itself. Besides this, recent work has not been limited to basic reconstruction algorithms but also focus on issues like mesh generation, electrode modelling, and visualization and error detection. Such advancements are facilitated by using modular components which could be plugged into a selection of reconstruction algorithms. EIDORS software has been completely restructured with the aim of providing an

extensible software base designed to support community use, contribution and modification.

Such modifications have been released as EIDORS version 3 (currently at release 3.1), which includes the following features:

Multiple algorithm support: EIDORS V.3 has been redesigned to allow flexibility of using multiple algorithms. We feel that this capability is becoming more important with a trend toward meta-algorithms in EIT, such as algorithms for detection of errors.

• *Generalized model formats*: One limitation of previous versions of the EIDORS software was, designing for specific configuration, stimulation and measurements patterns only. While it was possible to use this software for more general configurations, this was a fairly daunting task. In the interest to support the wide variety of EIT measurements and algorithms, EIDORS provides a general model format (i.e. the **fwd_model** structure). Beneficially, several utility functions are provided to create required model configurations. This format specifies the system model, sensor positions, conduction pattern and stimulation, and all supported algorithms are able to reconstruct images based on data provided in these formats.

• *Interface software for common EIT systems*: Useful functions are provided (in the interface directory) to data from hardware structure in the useful format. Currently, EIDORS will detect if data do not match the specified protocol in the **fwd_model**, but is not (yet) able to automatically convert the data. At this point it has only been possible for the developers to offer support for AT hardware that they have access to. There is a hope that EIDORS will soon attract contributions from software developers who have access to other hardware systems.

• *Usage examples*: It is seen that researchers typically base new software on demonstration examples. To avail this, several simple to more complex usage examples are provided for image reconstruction in two and three dimensions using various image reconstruction algorithms and combinations of algorithms.

• *Test suite*: Software is difficult to test. While little work has been done specifically on testing numerical software for inverse problems, we believe that such tests are even more difficult. EIDORS has begun to implement a series of regression test scripts (in the tests directory) to allow automatic testing of code modifications. For

example the function **calc_jacobian_test.m** validates a function to calculate the Jacobian against an approximation of the Jacobian using the perturbation method.

• *Open-source license*: EIDORS is licensed by the GNU General Public License [41]. Users are free to modify and distribute their modifications. Every modification must include source code, or instructions of how to obtain it. EIDORS can be used in commercial way, as long as the modifications for EIDORS and source code are available.

• *Sourceforge hosting*: To allow collaborative development, EIDORS is hosted by sourceforge.net available at http://eidors.org or http://eidors3d.sf.net. Download of Software is available as packaged released versions (version 3.1, released on 24 Jan 2006), or the latest developments may be downloaded from the Concurrent Versions System (CVS). Sourceforge hosting allows for collaborative development for group members, while permitting read-only access to everyone. To become a member of the developer group, new contributors should contact the authors. One concern with a distributed software project is the possibility of conflict because of disparate authors working on the same module. Version control software such as CVS is widely understood to facilitate collaborative development, and manage software version conflicts [42].

• *Language independence*: (Octave and MATLAB) EIDORS is originally written for MATLAB. Whereas, it's eventual goal is to support multiple mathematical software packages. Few progresses have been achieved, and EIDORS version 3 works also with Octave [43], although some advanced graphics functions still works onMATLAB (version > 6.0). Support for Octave was inspired for two major goals: first, it provides a free software platform which can motivate the development of embedded and commercial applications of AT which are currently limited by the MATLAB, and secondly, Octave provides an open source platform to match the open source nature of EIDORS.

• *Pluggable code base*: In order to provide user modifications, EIDORS has been designed to provide some of the benefits of object-oriented (OO) software [44]: encapsulation, abstraction, inheritance and polymorphism. Such design uses function pointers to allow addition of new modules and controlling which parts of functions are executed. EIDORS is thus able to offer the OO features of packaging and polymorphism, while not encapsulation or inheritance.

• *Automatic matrix caching*: In order to raise performance of image reconstruction software, it is essential to save and reuse values of computational variables and image priors. Such caching complicates the software implementation, and potentially leads to errors. In order to simplify and ease the design, EIDORS offers an ability to automatically detect when the calculation requires a value previously calculated, and will automatically retrieve that previous value.

Such capability helps software based on EIDORS to be more clear and easier to decompose into functional modules.

• *Enhanced Finite Element Modeling and Graphical output*: Reconstruction of Image, especially in 3D, needs functions to show high quality graphical representations of the images. EIDORS provides list of functions for image presentation using the Matlab graphics features, also functions to display images using the VTK visualization program [45], after exporting the data to a vtk file. **Show_fem.m** displays a three dimensional model of the finite element mesh. All EIDORS graphics functions now use a single colour mapping function **calc_colours.m**, which allows global modification of all image coloring using a global variable **eidors_colours**.

3.2 Software Architecture

This section describes the structure of EIDORS objects and its relationship to the Following finite element models and numerical functions:

3.2.1 Object structure

EIDORS software consists of four primary objects: **data, image, fwd_model, inv_model**. Each object is represented as a structure. Every object has a name and type. The name can be arbitrary; it is displayed by the graphical functions, and could also be helpful to distinguish objects in a user specified function. The type is used to identify the object type (i.e. image, data etc.)

3.2.2 Forward Model (fwd_model):

The most useful EIDORS object is the **fwd_model**, which is designed to represent the finite element model (FEM), sensors positions and properties, and stimulation patterns, as well as it describes the functions to solve the forward problem of the model. The FEM is described by the field nodes ($V \times D$) D), elements ($N \times (D +$

1)), boundary ($B \times D$), where V is the number of vertices, N is the number of elements, B the number of elements near the boundary, and D the model dimension (D = 2 for 2D and D = 3 for 3D). The ground node is the vertex number attached to ground. The sensors are defined by a vector (S × 1) of sensor fields. Each of s sensor objects has field's z_contact (scalar) and nodes (vector) which represent the (possibly complex) contact impedance and vertices to which that sensor is connected.

A point element would have a single sensor nodes field with z_contact = 0 while an sensor with a complete element model would have multiple vertices specified in nodes and z_contact > 0. Eventually EIDORS does not require the electrode model to be the same for all elements in a **fwd_model.**

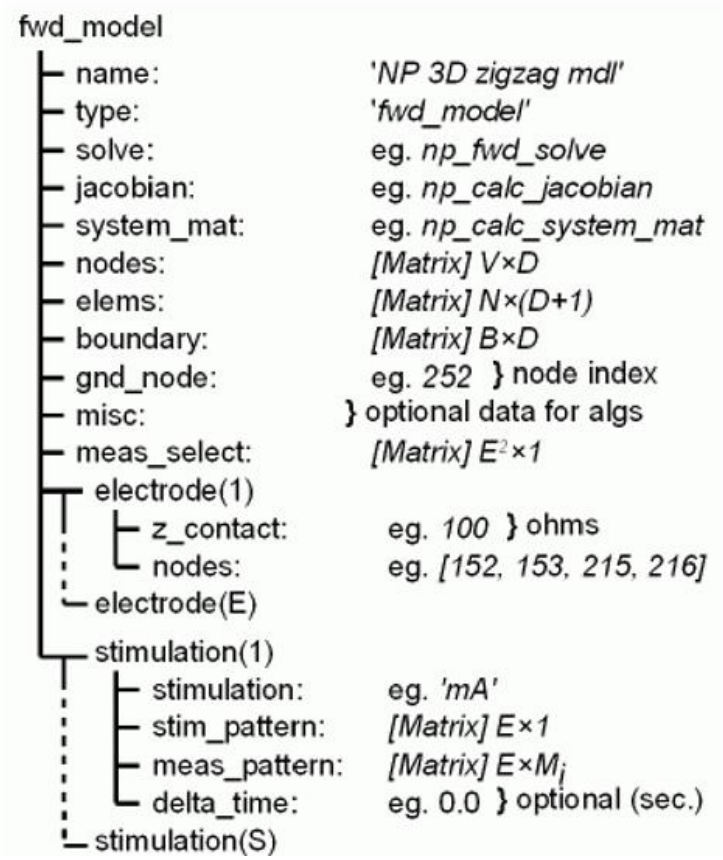

Figure 3.1: The Structure of the EIDORS Forward Model Object.

Using these sensor, sequences of P stimulation patterns are used and measurements performed such that, to generate a frame of data. Stimulation patterns are defined by a vector (P × 1) of stimulation fields. Each stimulation object has fields stimulation, **stim_pattern**, and **meas_pattern**. The stimulation is the quantity stimulated into the elements. Typically, AT systems inject sound (in decibels “db"), but the quantity could be voltage (or luminous intensity in an optical tomography system). Each stimulation object also has an optional **delta_time** field, representing the time increment between measurements at particular stimulation and the beginning of the measurement frame. Such data may be used to perform Kalman filtering, for example. **Meas_pattern** is a (sparse) matrix (S × Mi) representing the Mi measurement patterns for stimulation i. Every column of this matrix represents the amplification of the signal at each element for a single measurement pattern. EIDORS does not necessitate that the number of measurement patterns always be equal for each stimulation pattern. The total number of measurements per frame is M=ΣMi.

For many AT systems, an adjacent stimulation pattern is used with no measurement taken at present stimulation element, given M = S × (S− 3). For a 16 sensor system, this gives 208 measurements (or, considering reciprocity, 104 independent measurements). One practical consideration is that many AT systems store data as a matrix of size (S2×F) where F is the number of data frames. In this case S2 = 256 of which 3×S = 48 measurements in each frame yield zero. In order to allow easy use of EIDORS with such systems, the optional field **meas_select** (S 2× 1) is defined for the **fwd_model**. Such field contains a 1(one) in each position corresponding to a used measurement pattern in the frame (thus **meas_select** will have M ones). EIDORS provides several utility functions to define the fields of the **fwd_model** for common patterns, e.g. **mk_circ_tank.m, mk_stim_patterns.m** and **mk_common_model.m** functions. These functions allow easy definition of circular and cylindrical FEM models with rings of elements and adjacent stimulation protocols.

The **fwd_model** consists of three function pointers to allow solution of any forward problem, **solve, jacobian** and **system_mat**. Each field has the function name (as a string) or a function pointer to calculate these quantities. In each case, these quantities are solved using the utility functions **fwd_solve()**, **calc_jacobian()** and **calc_system mat()**.

For example, in a **fwd_model** object **fmdl**, we may calculate the system matrix, **Smat**, using:

Smat = calc_system_mat(fmdl);

This code will call the appropriate function and also manage the caching of the computed result. In this case, if a system matrix has previously been computed for any **fwd_model** object with the same values as **fmdl**, then the previous result will be returned, without the computation function being called.

3.2.3 Data

An EIDORS data object contains a frame of measurement or simulated data. The required fields are the actual frame data, **meas**, and the acquisition time, in seconds after the epoch. In a specific application, time may be defined with respect to a start point, such as the start of the experiment, or may be set to 0 or -1 for unknown times or simulated data.

```
data
├ name:          'measured by XYZ'
├ type:          'data'
├ time:          [scalar]          } unix time
├ meas:          [Matrix] M×1
├ configuration: eg. '16 ring elecs' } optional
└ fwd_model:     fwd model structure
```

Figure 3.2: The structure of the EIDORS Data Object.

The **meas** field is a $M \times 1$ matrix where M is the number of measurements for each data frame (the sum of number of measurements for each stimulation pattern). The data for **meas** is ordered such that the measurements for **stimulation** are first.

Data can be loaded into EIDORS by calling the **eidors_readdata()** function, which provides an interface to the storage formats. The data object may also contain two optional fields, configuration and **fwd_model**. Detailing of **fwd_model** allows EIDORS to validate that the data are being interpreted correctly, and being reconstructed as correct model. The configuration is a user specified string with a similar function; software may assign a value to this field in order to distinguish data objects.

3.2.4 Image

The EIDORS image object conveys the reconstructed or simulated conductivity values. The field **elem_data** ($N \times 1$) is the value of the image elements in the finite element model (in the field **fwd_model**).

```
image
├ name:        '3D simulation'
├ type:        'image'
├ elem_data:   [Matrix] N×1
├ node_data:   [Matrix] V×1  } nodal images
└ fwd_model:   fwd model structure
```

Figure 3.3: The structure of the EIDORS Image Object.

For example, given an **inv_model** object **imdl**, we may express image reconstruction by (assuming difference AT, and data objects data1 and data2):

```
img= inv_solve( imdl, data1, data2 );
```

Similarly, in order to simulate data object **datasim** from a simulation image **imgsim**, we may write:

```
datasim = fwd_solve(fmdl, imgsim);
```

3.2.5 Reconstruction

The reconstruction of image is done by the software called EIDORS which Provides free software algorithms for forward and inverse modelling for AT. Many reconstruction algorithms are available for use like back-projection method, Newton's method, GREIT (Graz consensus Reconstruction algorithm for EIT) [46].

To run the EIDORS software package on computer we required MATLAB (≥7.0) or Octave (≥3.6), Netgen Mesher (optional) required if we want to generate customized meshes. The software is very flexible and provides many regularization algorithms to improve the quality of the final solution. The software also provides wide variety of hyper parameter selection which is very crucial when solving the model problem.

3.3 EIT Processing

The processing of the AT data was accomplished using the EIDORS toolkit for MATLAB.. The first step in solving for the model distribution is to create a finite element model of the core and elements; Figure 3.4 is an example of 16 element and 1 ring model. With this finite element model, the forward problem was solved assuming a system of homogeneous resistance for the data.

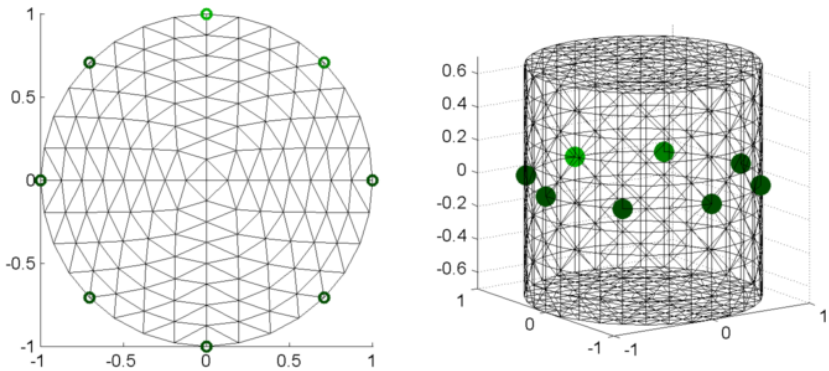

Figure 3.4: Finite Element Mesh and Electrodes used to Solve Forward Problem

The next step is to load the real data set and solve the inverse problem. The inverse problem was solved using the different methods, which the EIDORS toolkit offers and other regularized nonlinear solvers to obtain a unique and stable inverse solution. After solving for the resistivity distribution the final image is reconstructed and displayed.

CHAPTER FOUR

HARDWARE DESCRIPTION

4.1 Model Components

Components of hardware are assembled so as to get and process the data that collected from 8 receivers which later be used to image reconstruction. Arrangement of components is shown in block diagram figure 4.1.

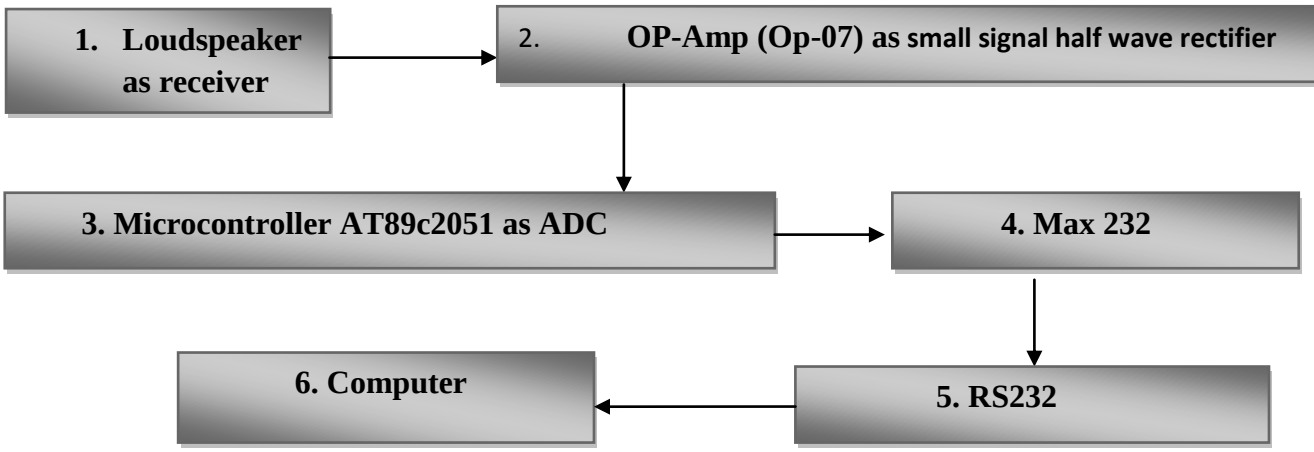

Fig. 4.1 Block diagram representation of the system model

4.1.1 Loudspeaker

Loudspeaker used as sound transducer which can be called as a “sound sensor” or “receiver”. It generates an electrical analog output signal and it is proportional to the “acoustic” sound wave acting upon its flexible diaphragm. Impedance of used speaker is 8Ω. Its process is similar to microphone. Loudspeaker uses electromagnetic induction to convert the sound wave signal into electrical signal. As the sound wave strikes flexible diaphragm, the diaphragm moves back and forth in action to the sound pressure acting upon it, which is causing the attached coil of wire to move within the magnetic field of the magnet. This movement of coil within the magnetic field causes a voltage to be induced in it and is defined by faraday’s law. Resultant output analog voltage signal is proportional to acoustic wave pressure. Analog signal produced so is of small amplitude and 90° out of phase to sound signal. So pre-amplification is required. The frequency response of loudspeaker is better than of microphone but the average quality of loudspeaker is not that much good as of microphone.

4.1.2 OP-07(Operational amplifier)

Operational Amplifier is used to amplify the weak analog output signal which is produced by loudspeaker transducer. OP-Amp is used as positive small signal half wave rectifier. We are using OP-Amp OP-07 because of its some of its some useful feature. OP-07 is having very low input offset voltage and high open loop gain which makes it useful for high gain applications. It is having high input voltage of ±13V with high CMRR of 110dB. With temperature and time variation stability of offset and gain is excellent [47].

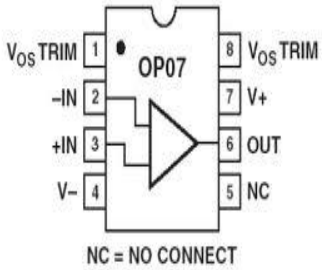

Fig.4.2 OP07 pin description

4.1.3 Microcontroller AT89c2051

Purpose of using specifically this microcontroller (AT89c2051) is having inbuilt comparator. AT89c2051 is a 20 pin IC, high-performance CMOS 8-bit microcomputer, with features: 2K bytes of Flash, 128 bytes of RAM, a precision analog comparator, on-chip oscillator, clock circuitry, 16-bit timer/counter. AT89c2051 is used to design ADC using slope integration ADC technique with some active and passive devices. BJT's, pnp for linear charging and npn is used as current mirror source for stability. And tantalum capacitor used to store and discharge voltage. The voltage on the capacitor as a function of time is given by the exponential equation:

$$VC = VCC\ (1\text{-}e\ \text{-}t/RC)$$

Where, VC is the voltage on the capacitor at time t, VCC is the supply voltage and RC is the product of the values of the resistor and capacitor [48].

4.1.4MAX 232

MAX 232 is a 16 pin IC that operates on single 5V supply, to make proper level converter and to establish the communication between microcontroller and PC. It is integrated with two drivers and two receivers that meet all specifications under 232-F standards.

This IC has two TTL/CMOS inputs on pin no. 11 & 10 whose inputs are pulled for VCC and their respective RS 232 output are on pin #14& 7.

Table 4.1: Function of each driver

TXin	Txout
0V	+12V
5V	-12V

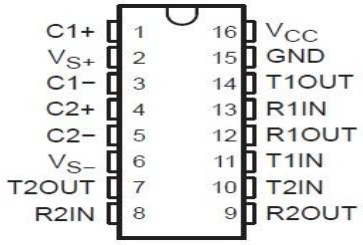

Fig 4.3 pin description of MAX 232

This IC has two RS232 receiving inputs pin on #13& 8. Their respective CMOS /TTL outputs are on pin # 12 & 9.

Table4. 2: Function of each receiver

RXin	Rxout
-12V	5V
+12V	0V

4.1.5 IC 74HC244 (Tri-state Octal Buffer/ line Driver)

74HC244 is an 8-bit buffer/ line driver with 3-state outputs. This device has two active low output enable (1OE and 2OE), each controlling four of the 3-state buffer. Instead of providing clock frequency and reset circuitry to each microcontroller with using lots of components, used a single IC (74HC244), by making reset circuitry and clock frequency output of only one microcontroller as input to IC and out output of IC is provide to rest of microcontrollers. Just with a single IC, cost of hardware reduces.

Table 4.3 TRUTH TABLE for 74HC244

INPUT		OUTPUT
nOE	nAn	nYn
L	L	L
L	H	H
H	X	Z

L: low voltage level; H: high voltage level; x: unknown state; Z: high impedance state

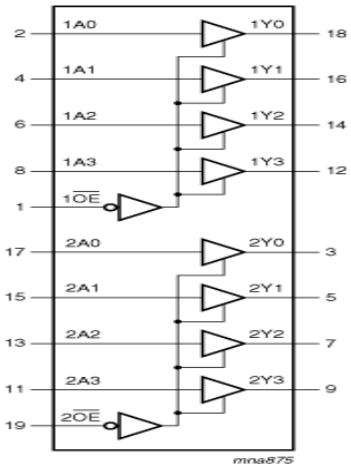

Fig. 4.4Pin description of 74HC244

4.1.6 IC SN7407 (HEX BUFFERS/ DRIVERS)

IC SN7407 is a TTL hex buffers/drivers with open-collector high-voltage outputs for interfacing with high current loads such as lamps, relays and with high level circuits (MOS). Boolean function of this device is Y=A. This IC is compatible with TTL families. In the schematic diagram of IC inputs are clamped with diodes to minimize the transmission line effects. Typical propagation delay time is of 14 ns and average power dissipation is 145 mW .

Purpose of using this IC in is to connect each microcontroller with MAX 232N to make it compatible with PC.

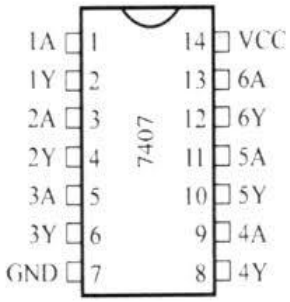

Fig 4.5 pin description of 7407 [49]

Features of SN 7407:

- High sink current capability.
- Convert TTL levels to MOS levels.
- Inputs fully compatible with most TTL circuits.
- Clamping Diodes at input simplify the system design.

4.2 Tomography Controller

The Tomography Controller (TC) is 8051 microcontroller based control system which uses data Acquisition System and the Reconstruction algorithm. It is the roll of the TC to switch between sensors while retrieving data. The main part of the TC circuit is the 8-bit microcontroller (AT89c2051) which is used for data collecting from the sensors and digitize the received data. The final part is the serial communication (RS232) for the communication between the TC and the computer.

The baud rate of 9600 is selected to send the data to computer. The software for

controller and data acquisition units was developed in the assembly language of microcontroller 8051. The acquired data was serially communicated to the Visual Basic 10.0 platform based program, this user friendly VB software allows one to select the name and location of the output data file.

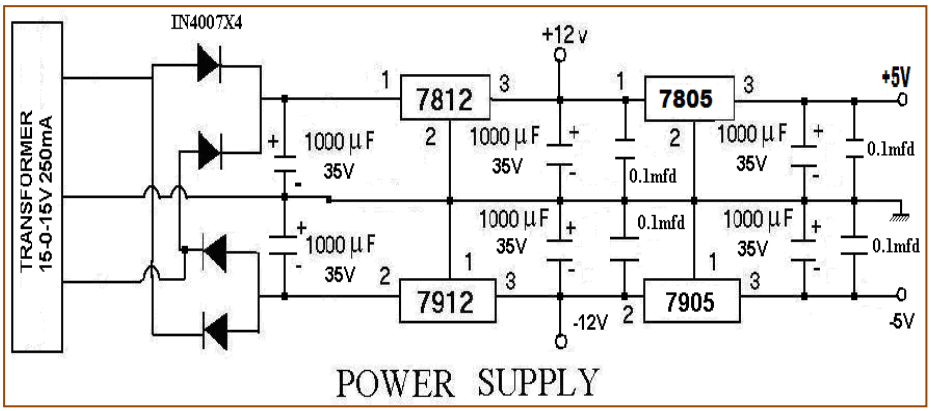

Fig 4.6 Block diagram of power supply. Designed in Diptrace schematic software

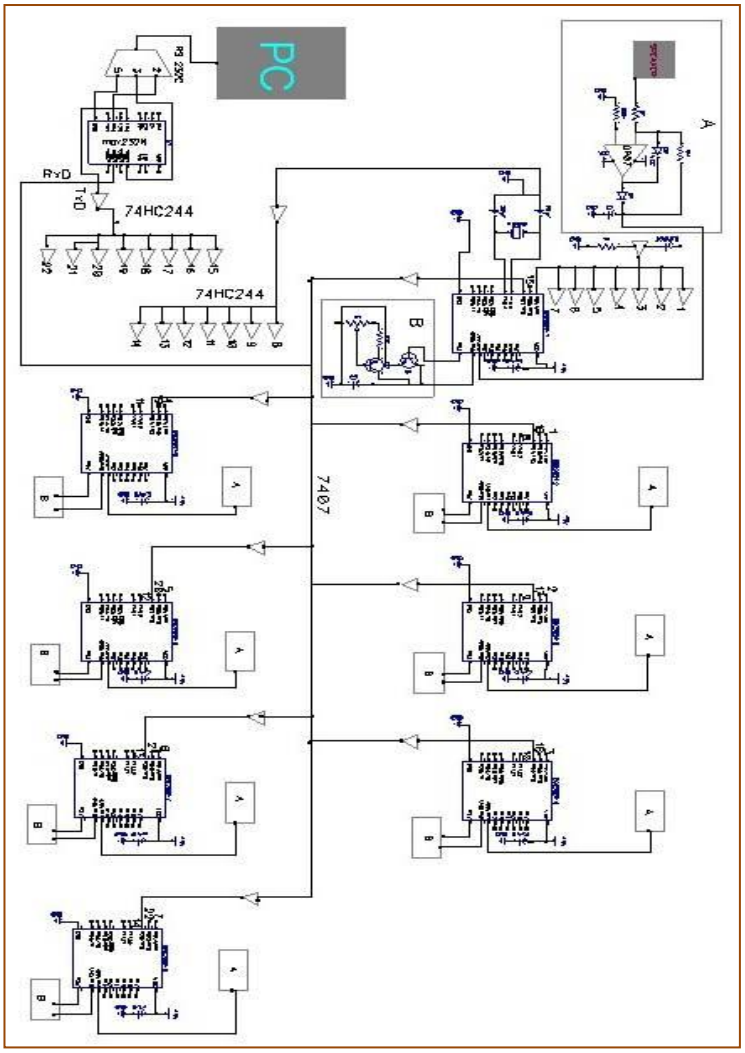

Fig 4.7 Block diagram of system model. Designed in Diptrace schematic software

CHAPTER FIVE

RESULTS AND DISCUSSION

5.1 Results

The system is tested in the reverberation chamber, with a sound source placed at the center of the room and sensors are placed around the source at some distance. Figure 5.1 shows the developed PCB model of components and figure 5.2 shows the speaker as sensor which takes the readings of sound pressure level (SPL) from the source at different frequencies. The data obtained by the model is when put in the software codes of Visual Basic, results are formed and prepared in the Microsoft excel sheet.

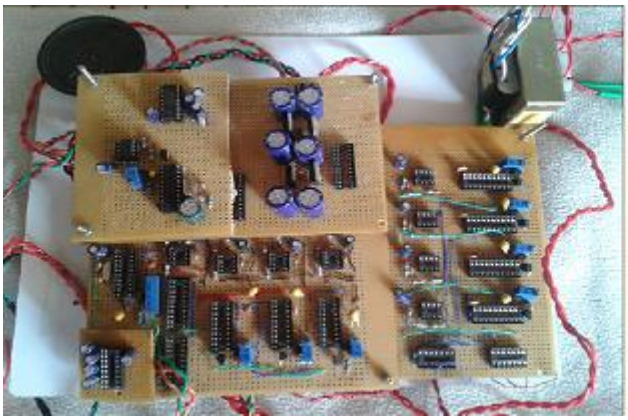

Fig 5.1 image of developed system

Fig 5.2 speaker as a sensor

A set of configurations was devised for the use of system model under different operating conditions given below:

A. Sound source is made to work at different sound power levels, ranging from 65W – 75W. At different sound power levels, the observed sound pressure level is different at different locations of sensors.
B. The operated frequency range of the sound source is varied in the range of 125 Hz- 10000Hz. At variable frequency range the obtained results are helpful in drawing the conclusion of the system model.

The obtained result chart standard deviation at different frequencies is shown in table 5.1. Each of the frequency applied results in sound power level change and hence the SPL in changed at the 8 sensors.

Table 5.1 Results obtained of standard deviation at variable frequencies

Frequency (Hz)	1	2	3	4	5	6	7	8	Standard Dev	SPL
125	74	74.3	73.5	73.3	73.1	72.1	72	74.6	0.95	73.36
160	71.7	71	71.2	72.2	70.3	70.7	69.7	72.1	0.87	71.11
200	73.6	72.4	73.2	73.6	72.2	72	74.7	73.8	0.93	73.19
250	73.5	73.5	72.3	71.5	70.7	72.3	72.8	72.9	0.97	72.44
315	71.5	71.6	70.2	70.6	71.2	70.2	70.2	71.4	0.63	70.86
400	72	72.2	72.1	71.7	72.1	72.1	70.9	71.5	0.44	71.83
500	71.3	71.7	71.3	71.4	71.7	71.7	71.8	72.4	0.36	71.66
630	71.6	71.1	70.9	71.1	71.3	71.2	71.1	71.8	0.30	71.26
800	73.1	72.7	72.3	72.8	72.2	72.2	72.1	73.9	0.61	72.66
1000	74.3	73.7	73.3	73.5	73.3	73.1	73.1	74.2	0.47	73.56
1250	75.8	75.3	74.4	74.6	74.2	74.4	74.4	75.6	0.63	74.84
1600	74.1	74.9	74.5	74.6	74.3	74.2	74.6	75.2	0.37	74.55
2000	73.6	73	73.2	73.2	73.2	73.1	73	74	0.34	73.29
2500	71.6	71.5	71.3	70.9	70.8	71	70.9	72	0.42	71.25
3150	70.4	70.3	70.4	70.2	69.7	69.8	70.1	70.8	0.35	70.21
4000	69.9	69.4	69.4	69.3	69.1	69.2	69.3	70	0.33	69.45
5000	68.4	68.1	67.5	67.5	67.6	67.5	67.6	68.6	0.45	67.85

From the results obtained at particular frequency by the sensors as SPL at 8 locations, formula for standard deviation (SD) is applied to calculate SD. These obtained SD's at different frequencies are examined and observed if they satisfy the criterion of SD variation of ± 1.5 , to validate the reverberation chamber.

This is the used SD formula:

$$\sigma = \sqrt{\frac{1}{N}\sum_{i=1}^{N}(x_i - \mu)^2}$$

Here N is the number of events, i.e. 8 sensors, μ is the calculated average of the 8 SPL values, x_i is the individual SPL value, where i ranges from 1- 8.

As it is seen from the data Table 5.1 that the SD at each frequency lays in the limit range of ± 1.5, so the proposed method is an effective way validate the reverberation chamber. Now to compare the present method with the conventional method SPL obtained by both the methods are compared and results of comparison can be shown by the graphs. Table 5.2 show the results obtained by conventional methods at some particular frequencies.

Table 5.2 Results obtained by conventional method using microphone.

Frequency (Hz)	1	2	3	4	5	6	7	8	Standard Dev	SPL
125	74.8	72.4	71.5	75.6	69.4	72.1	74.2	71.9	1.20	73.36
250	73.5	73.5	70.3	74.1	70.4	71.8	73.3	70.2	0.97	72.44
500	73.1	71.7	69.9	72.7	70.9	70.4	73.9	70.6	1.34	71.66
1000	74.3	73.7	72.4	74.2	71.2	73.1	73.5	72.7	0.86	73.56
5000	70.1	68.1	67.5	71	67.6	67.1	69.7	65.9	1.21	68.38

Here in the both the tables i.e. (table 5.1 and 5.2) the SPL column is the sound power level of the sound source and the columns 1 – 8 are the obtained sound pressure levels by the sensors. In order to compare both the methods, sound pressure levels in two methods will be compared, and that will indicate the level of dissipation and distortion of sound waves from a sound source in the chamber. For fine results and in order to find the better method, the one with the less distortion will be proven as more accurate method. The reason of taking sound pressure level as basis of comparison is that, the present method tends to remove the presence of reading taking person from the room, which is counted as the source of disturbance or distortion in the room. Less is the source of distortion in the room more accurate will be the distribution pattern of sound waves from the source.

Table 5.3 Comparison graph of conventional system and proposed automatic model

Applied Frequency	Graph representation of conventional method	Graph representation of automatic purposed model
At 125HZ	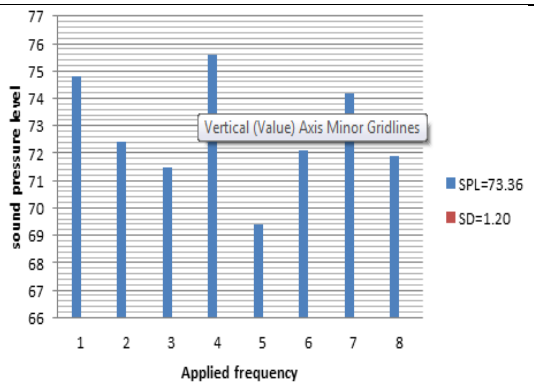	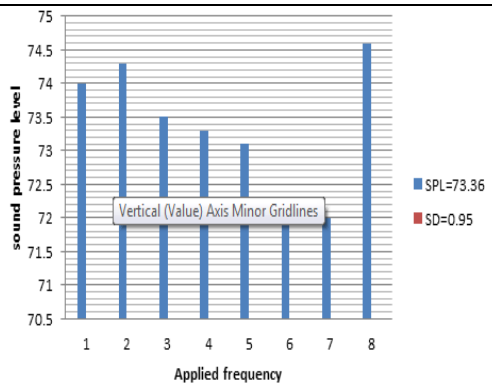
At 250 HZ	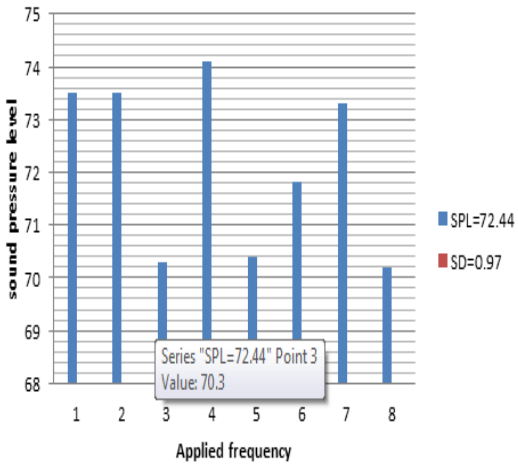	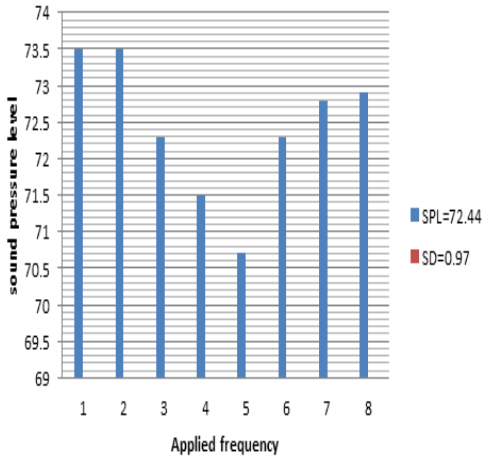
At 500 HZ	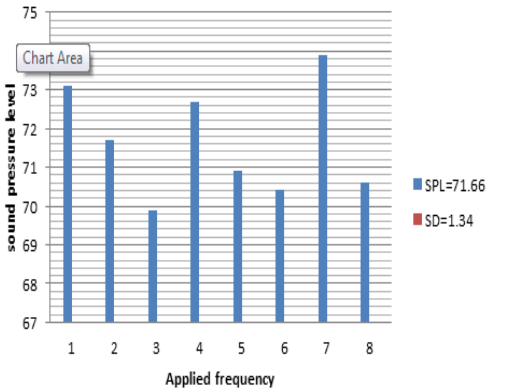	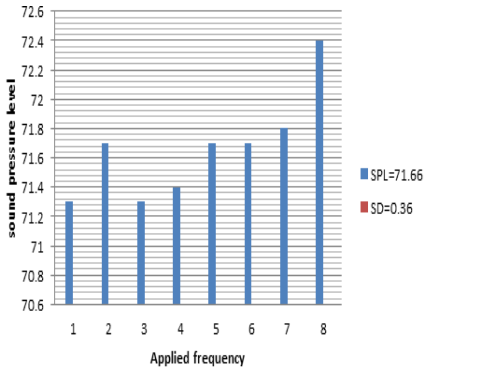

At 1000HZ	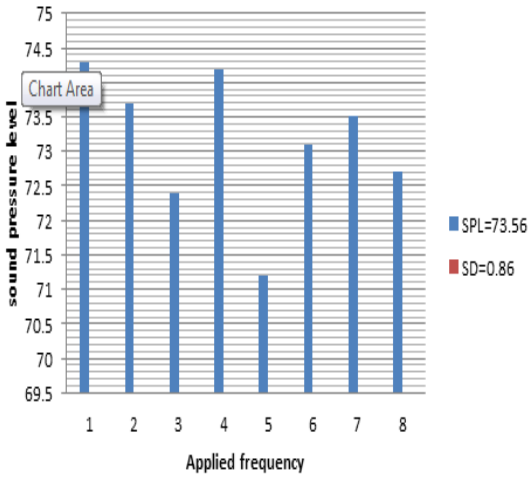	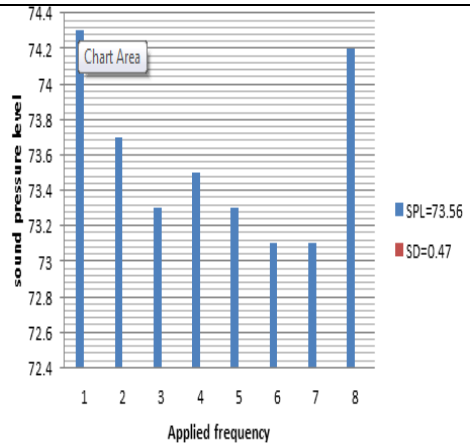
At 5000HZ	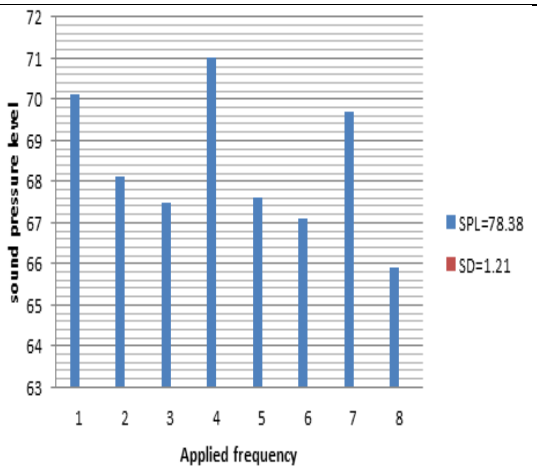	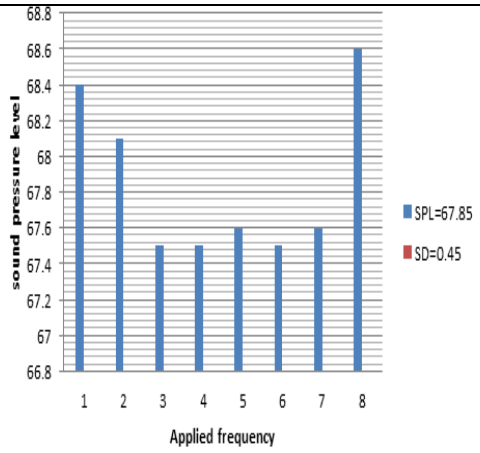

5.2 Conclusion

When the above graphs were compared, it is found that the SPL of the proposed model shows better scattering pattern, as the deviation is less than that of the conventional method. Also From the above comparison graphs, it can be concluded that the present system model shows better results than conventional method. So the traditional method used in the laboratory can be replaced by this new model.

The developed system finds application in the field of biomedical instrumentation, nondestructive testing, flow measurement, geophysical prospecting cross borehole measurement etc.

Algorithms used here can also be used for following purposes:

1. Electrical impedance tomography
2. Used along with acoustic as well as seismic measurements for determination of sub surface cavities.
3. Used as a prototype in the laboratory for demonstration.

CHAPTER SIX

FUTURE WORK

6.1 Variable Height

This type of system that we are using in our project after calibration at different amplitudes and heights of sensors can be utilized for Acoustic 3D Mapping of the chambers (Reverberation and Anechoic) and thereafter this technology can be transferred to **National Metrology Institutes (NMI)** of other countries of the world.

6.2 Increasing sensor Numbers

This system model is made as 8 sensor configuration and can be made for more configurations i.e. for 16 or 32 sensors. And that could be even more effective method.

6.3 Clinical Experiments

For the system to be useful in a medical environment, it is necessary to carry out experiments to determine whether medical conditions can be accurately assessed. Currently it has been stated [50] that existing AT methods has not been as effective as standard X-radiography in assessing pulmonary edema. As this is a likely application for AT, it is important that tests should be carried out to determine the effectiveness of absolute imaging in this and other applications.

CHAPTER SIX

REFERENCES

[1] Merriam-Webster dictionary

[2.] Colston Jr, Bill W., et al. "Imaging of the oral cavity using optical coherence tomography." (2004): 32-55.

[3] Natterer, Frank, and Frank Wubbeling. "A propagation-backpropagation method for ultrasound tomography." *Inverse problems* 11.6 (1995): 1225.

[4] Pascual-Marqui, Roberto D., Christoph M. Michel, and Dietrich Lehmann. "Low resolution electromagnetic tomography: a new method for localizing electrical activity in the brain." *International Journal of psychophysiology* 18.1 (1994): 49-65.

[5] F. Natterer, 'The mathematics of computerization tomography', Wily, New York, 1986.

[6] Schubert, Frank. "Basic principles of acoustic emission tomography." *Journal of Acoustic Emission* 22 (2004): 147-158.

[7] Bregman, N. D., R. C. Bailey, and C. H. Chapman. "Crosshole seismic tomography." *Geophysics* 54.2 (1989): 200-215.

[8] Tromp, Jeroen, Carl Tape, and Qinya Liu. "Seismic tomography, adjoint methods, time reversal and banana-doughnut kernels." *Geophysical Journal International* 160.1 (2005): 195-216.

[9] Liang, Shanqing, et al. " Evaluation of acoustic tomography for tree decay detection." *Series: Conference Proceedings*. 2008.

[10] I. Jovanovic,, "inverse problem in acoustic tomography : theory and application." , PhD Thesis, 2008

[11] Li, Haiyue, Syogo Takata, and Akira Yamada. "Tomographic Measurement of Vortex Air Flow Field Using Multichannel Transmission and Reception of Coded Acoustic Wave Signals." *Japanese Journal of Applied Physics* 50.7 (2011).

[12] Duric, Nebojsa, et al. "Detection of breast cancer with ultrasound tomography: First results with the Computed Ultrasound Risk Evaluation (CURE) prototype."*Medical physics* 34.2 (2007): 773-785.

[13] Duric, Nebojsa, et al. "In-vivo imaging results with ultrasound tomography: Report on an ongoing study at the Karmanos Cancer Institute." *SPIE Medical Imaging*. International Society for Optics and Photonics, 2010.

[14] K.Nogami, A.Yamada, Jpn.J.Appl.Phys., **46**, 7B, pp.4820-4826 (2007).

[15] H.Li T. Ueki and A.Yamada, Jpn.J.Appl.Phys., **47**, 5, pp.3940-3945(2008).

[16] Akira Yamada, Jpn.J.Appl.Phys., **48**, 07GC01, pp.1-6 (2009).

[17] Woodward, Marta Jo. "Wave equation tomography." *Geophysics* 57.1 (1992): 15-26.

[18] Trampert, Jeannot, and Jesper Spetzler. "Surface wave tomography: finite-frequency effects lost in the null space." *Geophysical Journal International*164.2 (2006): 394-400.

[19] Montelli, R., et al. "Global P and PP traveltime tomography: rays versus waves." *Geophysical Journal International* 158.2 (2004): 637-654.

[20] Spetzler, Jesper, and Roel Snieder. "The Fresnel volume and transmitted waves." *Geophysics* 69.3 (2004): 653-663.

[21] Schomberg, Hermann. "An improved approach to reconstructive ultrasound tomography." *Journal of Physics D: Applied Physics* 11.15 (1978): L181.

[22] Andersen, Anders Hvid. "Ray linking for computed tomography by rebinning of projection data." *The Journal of the Acoustical Society of America* 81.4 (1987): 1190-1192.

[23] Norton, Stephen J. "Computing ray trajectories between two points: a solution to the ray-linking problem." *JOSA A* 4.10 (1987): 1919-1922.

[24] Andersen, Anders H. "A ray tracing approach to restoration and resolution enhancement in experimental ultrasound tomography." *Ultrasonic imaging* 12.4 (1990): 268-291.

[25] Ramananantoandro, R., and N. Bernitsas. "A computer algorithm for automatic picking of refraction first-arrival time." *Geoexploration* 24.2 (1987): 147-151.

[26] Li, Cuiping, et al. "An improved automatic time-of-flight picker for medical ultrasound tomography." *Ultrasonics* 49.1 (2009): 61-72.

[27] Kak, AVINASH C., and Kris A. Dines. "Signal processing of broadband pulsed ultrasound: measurement of attenuation of soft biological tissues." *Biomedical Engineering, IEEE Transactions on* 4 (1978): 321-344.

[28] Snieder, Roel, and Anthony Lomax. "Wavefield smoothing and the effect of rough velocity perturbations on arrival times and amplitudes. " *Geophysical Journal International* 125.3 (1996): 796-812.

[29] Bissantz, Nicolai, et al. "Convergence rates of general regularization methods for statistical inverse problems and applications." *SIAM Journal on Numerical Analysis* 45.6 (2007): 2610-2636.

[30] Ishimaru, Akira. *Wave propagation and scattering in random media*. Vol. 2 New York: Academic press, 1978.

[31] Keller, JosephB "Accuracy and Validity of the Born and Rytov Approximations*. " *JOSA* 59.8 (1969): 1003.

[32] Devaney, A. J. "Inverse-scattering theory within the Rytov approximation."*Optics letters* 6.8 (1981): 374-376.

[33] Devaney, A. J. "Inversion formula for inverse scattering within the Born approximation." *Optics Letters* 7.3 (1982): 111-112.

[34] Pratt, R. Gerhard, et al. "Sound-speed and attenuation imaging of breast tissue using waveform tomography of transmission ultrasound data." *Medical Imaging*. International Society for Optics and Photonics, 2007.

[35] Wang, Yilun, et al. "A new alternating minimization algorithm for total variation image reconstruction." *SIAM Journal on Imaging Sciences* 1.3 (2008): 248-272.

[36] Engquist, Björn, and Andrew Majda. "Absorbing boundary conditions for numerical simulation of waves." *Proceedings of the National Academy of Sciences* 74.5 (1977): 1765-1766.

[37] Roy, Olivier, et al. "Sound speed estimation using wave-based ultrasound tomography: theory and GPU implementation." *SPIE Medical Imaging*. International Society for Optics and Photonics, 2010.

[38] Vauhkonen M, LionheartWR B, Heikkinen L M, auhkonen P J and Kaipio J P,"A
MATLAB package for the EIDORS project to reconstruct two-dimensional EIT images" Physiol. Meas. 22 107-111, 2000

[39] Vauhkonen M, “Electrical impedance tomography and prior information”, PhD thesis, University of Kuopio, Finland, 1997.

[40] Polydorides N, “Image reconstruction algorithms for soft-field tomography”, Ph.D. Thesis, University of Manchester Institute of Science and Technology, U.K, 2002.

[41] Free Software Foundation, GNU General Public Licence Boston MA USA http:/www.gnu.org/copyleft/gpl.html , 1991.

[42] Cederqvist P, “Version Management with CVS”, Network Theory Ltd, Bristol, UK, 2002.

[43] Eaton J W, “Gnu Octave Manual”, Network Theory Ltd, Bristol, UK, 2002.

[44] Gamma E Helm R Johnson R and Vlissides J, “Design Patterns: Elements of Reusable Object- Oriented Software Addison-Wesley”, Boston, MA, USA, 1995.

[45] Ramachandran P, “Scientific data visualization with MayaVi Conf. SciPy: Python for Scientific Computing Pasadena”, CA, USA http://mayavi.sf.net/, 2003.

[46] A. Adler, W.R. B. Lionheart , ‘Uses and abuses of EIDORS: An extensible software base for EIT’.

[47] doc.chipfind.ru/nsc/**op07**.h [48] **www.atmel.in_Images_doc0524**

[49] www.datasheetdir.com/SN**7407**+Buffers-Drivers

[50] Holder DS, Biomedical applications of EIT: a shopping list for clinicians and engineers, presentation at the 5th European Community workshop on electrical impedance tomography, Barcelona 1993.